Supporting information

Spherical nanoflower-shaped Co-2MI with laccase-like activity for colorimetric detection of salbutamol

Lili Xu [a,b], Jianli Nan[a,c], Songxue Han[a,c], Youxing Fang[d]*, and Shaojun Dong [a,b,c]*

[a]*State Key Laboratory of Electroanalytical Chemistry, Changchun Institute of Applied Chemistry, Chinese Academy of Sciences, Changchun 130022, China*

[b]*University of Science and Technology of China, Hefei 230026, China*

[c]*College of Chemistry, Jilin University, Changchun 130012, China*

[d]*School of Chemical Engineering and Technology, Sun Yat-sen University, Zhuhai, 519082, China*

Corresponding author

*E-mail: dongsj@ciac.ac.cn; fangyouxing@mail.sysu.edu.cn

Experimental section

1. Reagents and Chemicals

2,2'-Bipyridine-4,4'-dicarboxylic acid (H_2BPDCA) was purchased from Sigma-Aldrich Trading Co., Ltd. Salbutamol sulfate (SAL), 2-methylimidazole (2-MI), 1,3,5-benzenetricarboxylic acid (H_3BTC), cobalt(II) nitrate hexahydrate ($Co(NO_3)_2 \cdot 6H_2O$), 2,4-dichlorophenol (2,4-DP), and 4-aminoantipyrine (4-AAP) were obtained from Shanghai Aladdin Reagent Co., Ltd. N,N-Dimethylformamide (DMF) and sodium chloride (NaCl) were purchased from Xilong Scientific Co., Ltd. Terephthalic acid (H_2BDC) was supplied by Shanghai Macklin Biochemical Co., Ltd. Laccase (from *Aspergillus* spp., 10,000 U g^{-1}) was obtained from Adamas Reagent. Glycine was provided by Sinopharm Chemical Reagent Co., Ltd. Glucose and sucrose were obtained from Beijing Chemical Works. Serine, threonine, and methionine were purchased from Shanghai PureM Biological Technology Co., Ltd. All chemicals were of analytical grade and used without further purification. Ultrapure water (resistivity ≥18.2 MΩ·cm) purified using a Millipore Milli-Q system was used throughout all experiments.

2. Apparatus

Scanning electron microscopy (SEM) images were obtained using a Zeiss Gemini Sigma 300 field-emission scanning electron microscope. Transmission electron microscopy (TEM) images were acquired using a Hitachi H-8100 transmission electron microscope operated at an acceleration voltage of 100 kV. UV–Vis absorption spectra were recorded on an Agilent Cary 60 UV–Vis–NIR spectrophotometer (Varian, USA). X-ray photoelectron spectroscopy (XPS) measurements were performed on an ESCALABMKII spectrometer (VG Co., UK) using Al Kα radiation as the excitation source. X-ray diffraction (XRD) analysis was conducted on a D8 ADVANCE diffractometer (Bruker, Germany) with Cu Kα radiation (λ = 1.5406 Å). Electron paramagnetic resonance (EPR) spectroscopy was performed on a Bruker EMXPLUS spectrometer. N_2 adsorption–desorption isotherms were measured using a NOVA 4200e surface area and pore size analyzer. Thermogravimetric analysis (TGA) was conducted on a Pyris Diamond TGA/DTA instrument (PerkinElmer, USA). Fourier transform infrared (FTIR) spectra were collected using a VERTEX 70 spectrometer (Bruker, Germany).

3. Synthesis of Co MOF Materials

Synthesis of Co-BTC [1]*:*

0.3718 g (2 mmol) of cobalt(II) acetate tetrahydrate ($Co(CH_3COO)_2 \cdot 4H_2O$) and 0.4203 g (2 mmol) of 1,3,5-benzenetricarboxylic acid (H_3BTC) were dissolved in 30 mL of DMF. The solution was ultrasonicated at room temperature for 20 min to ensure homogeneity and then transferred into a Teflon-lined autoclave for hydrothermal treatment at 140 °C for 24 h. After naturally cooling to room temperature, the product was collected by centrifugation and washed three times with ethanol and DMF. The

resulting purple powder was dried under vacuum at 60 °C for 8 h.

Synthesis of Co-BPDCA[2]*:*

1.4552 g (5 mmol) of $Co(NO_3)_2 \cdot 6H_2O$ and 0.6105 g (2.5 mmol) of H_2BPDCA were dissolved in 30 mL of a mixed solvent (H_2O:ethanol = 1:1) containing 0.3 g (7.5 mmol) of NaOH. The mixture was ultrasonicated for 20 min at room temperature and then transferred into an autoclave for hydrothermal reaction at 160 °C for 12 h. After cooling, the product was centrifuged, washed three times with ethanol, and dried under vacuum at 120 °C for 12 h.

Synthesis of Co-BDC [3]*:*

0.1426 g (0.49 mmol) of $Co(NO_3)_2 \cdot 6H_2O$ and 0.0814 g (0.49 mmol) of terephthalic acid (H_2BDC) were dissolved in 35 mL of DMF. After ultrasonic treatment for 20 min at room temperature, the solution was transferred to a Teflon-lined autoclave and reacted hydrothermally at 120 °C for 24 h. The mixture was cooled to room temperature, centrifuged, washed with DMF and ethanol, and dried under vacuum at 50 °C overnight.

Synthesis of Co-2MI [4]*:*

0.8731 g (3 mmol) of $Co(NO_3)_2 \cdot 6H_2O$ was dissolved in 60 mL of methanol, and 0.4926 g (6 mmol) of 2-methylimidazole (2-MI) was dissolved in 20 mL of methanol. The 2-MI solution was slowly added dropwise to the cobalt solution under continuous stirring, followed by an additional 5 min of stirring. The resulting mixture was transferred to an autoclave and heated hydrothermally at 120 °C for 12 h. After cooling, the precipitate was centrifuged and washed twice with ethanol and deionized water, then dried under vacuum at 60 °C overnight to yield a brown solid.

The corresponding characterization results are shown in Fig. S1. XRD patterns (Fig. S1d–f) reveal that Co-BTC, Co-BDC, and Co-BPDCA all exhibit good crystallinity and phase purity. SEM images (Fig. S1a–c) show distinct morphologies: Co-BTC presents an irregular micron-scale structure, Co-BDC forms a large stacked sheet-like morphology, and Co-BPDCA appears as tapered rod-like structures. As shown in Fig. S1g–l, the chemical composition and oxidation states of the Co-MOFs were analyzed by X-ray photoelectron spectroscopy (XPS). The full survey spectra (Fig. S1g–i) confirm the presence of Co, C, and O elements in all three materials, consistent with the expected MOF compositions. High-resolution Co 2p spectra (Fig. S1j–l) were deconvoluted to identify the oxidation states. Similar to Co-2MI, the Co $2p_{3/2}$ and Co $2p_{1/2}$ regions exhibit peaks attributable to both Co^{3+} and Co^{2+}, along with two shake-up satellite peaks. XPS analysis indicates that Co^{3+} is the dominant species in Co-BTC and Co-BPDCA, whereas Co^{2+} is more prevalent in Co-BDC.

4. Laccase-Mimicking Activity of Co MOFs and Comparative Study

Activity comparison:

A reaction mixture was prepared by mixing 50 μL of 4-AAP solution (2 mg mL^{-1}),

50 μL of 2,4-DP solution (2 mg mL^{-1}), and 800 μL of HAc–NaAc buffer (50 mM, pH 6.0). Then, 100 μL of Co MOF aqueous dispersion (1 mg mL^{-1}) or laccase solution (1 mg mL^{-1}) was added to the mixture. After incubation at 60 °C for 30 min, the reaction mixture was centrifuged (10,000 rpm, 3 min), and the absorbance of the supernatant was recorded at 510 nm.

Activity optimization experiment:

The effects of pH (4, 5, 6, 7, 8, 9, and 10), temperature (20, 30, 40, 50, 60, 70, and 80 °C), Co-2MI concentration (0.02, 0.05, 0.10, 0.15, and 0.20 mg mL^{-1}), gas atmosphere (N_2, air, and O_2), and reaction time (5, 10, 20, 30, 40, and 60 min) on the Co-2MI catalyzed oxidation of 2,4-DP were systematically investigated. As shown in Fig. S4a, the laccase-like activity of Co-2MI initially increased and then decreased with rising pH, reaching a maximum at pH 6. Within the temperature range of 30–80 °C, the catalytic activity also followed a similar trend—first increasing and then decreasing with temperature, with the optimal temperature determined to be 60 °C (Fig. S4b). For the effects of reaction time and catalyst concentration, as illustrated in Fig. S4c, the absorbance of the reaction mixture gradually increased over time and eventually reached a plateau, with the rate of increase diminishing progressively. To balance catalytic efficiency and experimental practicality, a reaction time of 30 min was selected as the optimal condition. Moreover, as shown in Fig. S4d, the absorbance increased with the concentration of Co-2MI and began to level off beyond 0.1 mg mL^{-1}. A sharp increase in activity was observed below this threshold, while only a slight improvement was seen with further increases in catalyst concentration. Therefore, 0.1 mg mL-1 of Co-2MI was chosen as the optimal dosage. Based on these findings, the optimized catalytic conditions were defined as follows: 0.1 mg mL^{-1} Co-2MI in a pH 6 buffer system, reacted at 60 °C for 30 minutes.

Stability Test:

Storage stability was assessed by measuring the laccase-like activity of Co-2MI after storage at room temperature for 0, 10, 20, and 30 days. As shown in Fig. S7a, the relative activity of Co-2MI remained nearly unchanged over the course of one month of storage, indicating excellent storage stability. Moreover, XRD and XPS analyses (Fig. S7b–d) confirmed that both the crystalline structure and the valence states of cobalt in Co-2MI showed no significant changes before and after the catalytic reactions. These results demonstrate that Co-2MI maintains good structural stability during use.

H_2O_2 Detection:

After the Co-2MI catalyzed oxidation of 2,4-DP, the supernatant was collected and mixed with 100 μL of ABTS (2.8 mg mL^{-1}) and 100 μL of HRP (0.05 mg mL^{-1}). The absorbance was recorded, then an additional 100 μL of 5 % H_2O_2 was added. The mixture was diluted threefold, and the absorbance was measured again. As shown in Fig. S3d, no H_2O_2 was detected, indicating that O_2 was reduced directly to H_2O rather than forming H_2O_2, which is consistent with the catalytic mechanism of natural laccase[5].

Radical-Scavenging Experiments:

Tert-butanol (TBA), sodium azide (NaN_3), and superoxide dismutase (SOD) were selected as quenchers for •OH, $^1O_2$, and $•O_2^-$, respectively. The control reaction contained no quencher; the experimental reactions each contained one quencher. All reactions were carried out in a total volume of 1 mL, with 50 μL of TBA, 50 μL of 1 M NaN_3, or 50 μL of SOD (1 mg mL^{-1}) added. After reacting at 60 °C for 20 min, mixtures were centrifuged and the absorbance of the supernatant was recorded.

5. Steady-State Kinetic Analysis of Co MOF with Laccase-like Activity

Steady-state kinetic analysis of the laccase-like activity was performed by varying the concentration of 2,4-DP while keeping the concentration of 4-AAP constant. Specifically, different concentrations of 2,4-DP (50 μL) were added to HAc–NaAc buffer (50 mM, pH 6.0, 800 μL) containing 4-AAP (50 μL, 2 mg mL^{-1}), followed by the addition of Co-2MI (100 μL, 1 mg mL^{-1}) or laccase (100 μL, 1 mg mL^{-1}) to initiate the reaction. The absorbance at 510 nm was monitored to determine the apparent initial catalytic rate.

The substrate concentrations and reaction rates were fitted to the Michaelis–Menten equation to obtain the kinetic parameters V_{max} and K_m:

$$V_0 = (V_{max}[s])/(K_m + [s])$$

where V_0 is the initial reaction rate, K_m is the Michaelis constant, V_{max} is the maximum reaction rate, and [S] is the substrate concentration.

6. Colorimetric Detection of Salbutamol

Colorimetric assay:

The one-step colorimetric determination of SAL is based on the 1:1 molar reaction between oxidized SAL and 4-AAP, producing a colored species with an absorption maximum at 556 nm. In a typical assay, 50 μL of 4-AAP solution (2 mg mL^{-1}) and 50 μL of SAL solution (2 mg mL^{-1}) were mixed with 825 μL of HAc–NaAc buffer (50 mM, pH 6.0). Then, 75 μL of Co-2MI dispersion (2 mg mL^{-1}) was added to initiate the reaction. After incubation at 60 °C for 30 min, the mixture was centrifuged and the supernatant's absorbance was measured at 556 nm.

For calibration, varying concentrations of SAL were reacted with Co-2MI (0.15 mg mL^{-1}) and 4-AAP (0.10 mg mL^{-1}) under the same buffer conditions. After 30 min at 60 °C, the absorbance at 556 nm was recorded. A calibration curve was constructed by plotting absorbance versus SAL concentration. The limit of detection was calculated as $3\sigma/b$, where σ is the standard deviation of the blank signal and b is the slope of the calibration line.

Effect of reaction parameters:

The influence of pH (4–10), temperature (20, 30, 40, 50, 60, 70 °C), Co-2MI

concentration (0.05, 0.10, 0.15, 0.20 mg mL^{-1}), and reaction time (10, 20, 30, 40, 60 min) on the Co-2MI catalyzed SAL assay was systematically investigated. As shown in Fig. S7a–b, the catalytic activity of Co-2MI exhibited the highest activity at pH 6 and 60 °C. The absorbance of the reaction system increased progressively with time until equilibrium was reached; notably, the absorbance increased sharply within the first 30 minutes and plateaued thereafter (Fig. S7c). Considering experimental efficiency, a 30-minute reaction time was deemed optimal. Fig. S7d shows that the reaction rate increased with increasing concentrations of Co-2MI, leveling off at 0.15 mg mL^{-1}. Based on these results, the optimized experimental conditions were set as follows: 0.15 mg mL^{-1} Co-2MI in a pH 6 buffer solution, reacting at 60 °C for 30 minutes.

Interference study:

Potential interferents including glucose, sucrose, glycine, serine, threonine, methionine, $CaCl_2$, NaCl, and KNO_3 were each added at fivefold the SAL concentration to the reaction mixture. The assay's selectivity was evaluated by comparing absorbance changes in the presence and absence of these species. As shown in Fig. S8, under identical testing conditions, the influence of these coexisting substances on the colorimetric reaction was negligible, with the activity of Co-2MI remaining above 90%. These results demonstrate that the proposed detection system possesses excellent anti-interference ability.

7. Detection of Salbutamol in Real Water Samples

The applicability of the proposed method was evaluated using the standard addition approach in untreated tap water. In a typical procedure, 50 μL of raw tap water, 50 μL of 4-AAP solution (2 mg mL^{-1}), and 75 μL of Co MOF dispersion (2 mg mL^{-1}) were mixed. Known amounts of SAL standard solution were then spiked into this mixture, and the volume was adjusted to 1 mL with HAc–NaAc buffer (50 mM, pH 6.0). After reacting at 60 °C for 30 min, the absorbance at 556 nm was measured. The recovery percentage and relative standard deviation for SAL in the tap water samples were calculated.

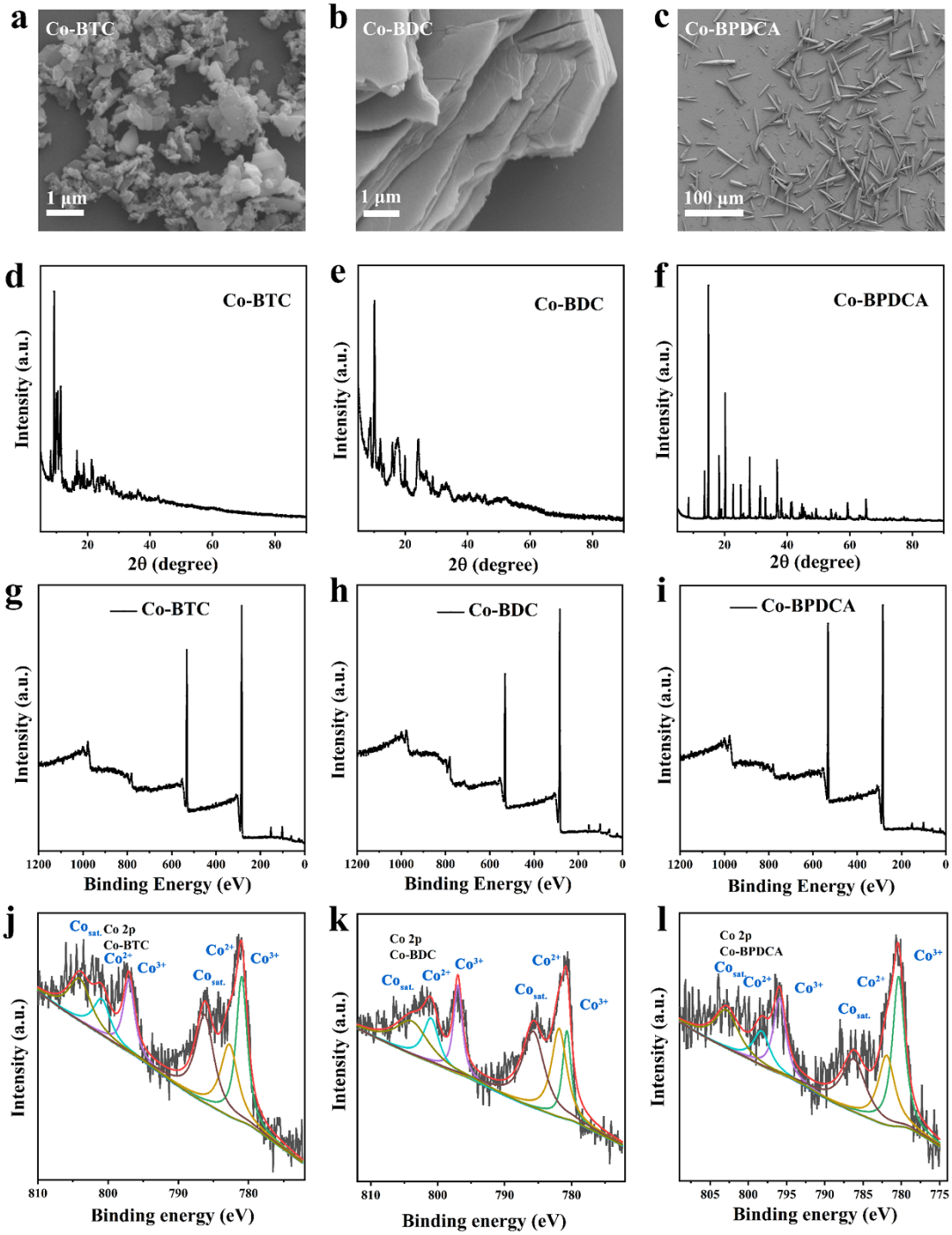

Fig. S1 (a, d, g, j) SEM images, XRD patterns, survey XPS spectra, and Co 2p spectra of the as-prepared Co-BTC; (b, e, h, k) SEM images, XRD patterns, survey XPS spectra, and Co 2p spectra of the as-prepared Co-BDC; (c, f, i, l) SEM images, XRD patterns, survey XPS spectra, and Co 2p spectra of the as-prepared Co-BPDCA

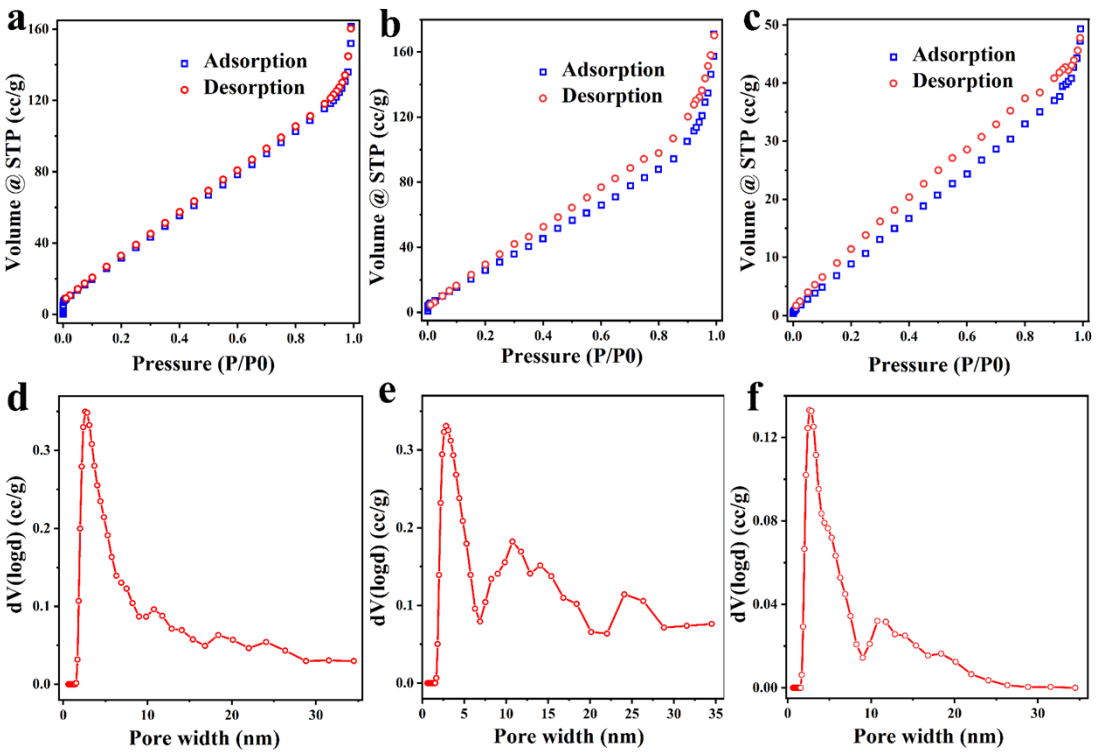

Fig. S2 BET surface area of Co-BTC (a), Co-BDC (b), Co-BPDCA(c) and average pore diameter of Co-BTC (d), Co-BDC (e), Co-BPDCA(f)

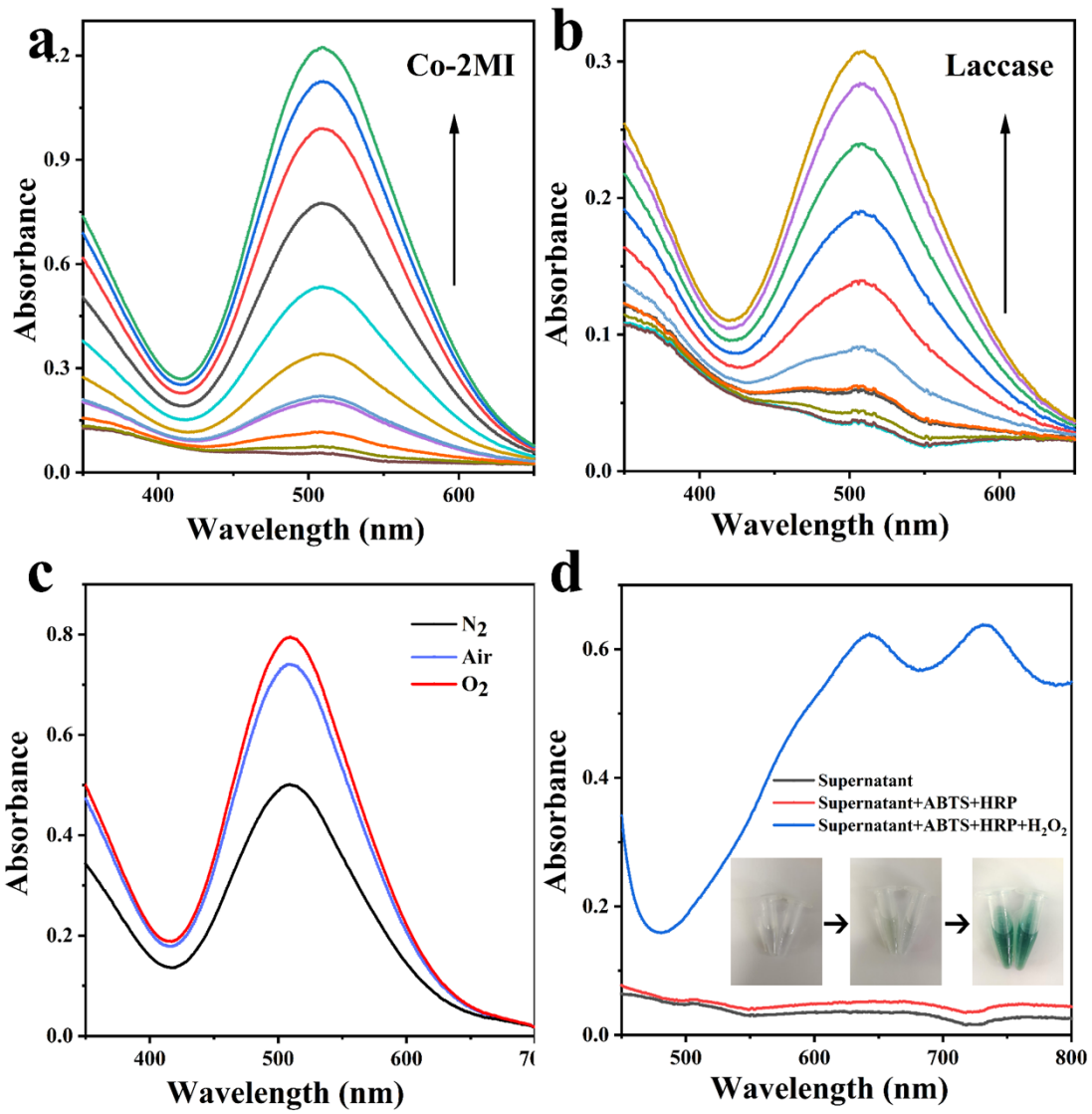

Fig. S3 Absorbance changes of the Co-2MI (a) and laccase (b) catalytic system with varying 2,4-DP concentrations; (c) Absorbance of the Co-2MI catalytic system under different saturation atmospheres; (d) Detection of the product H_2O_2

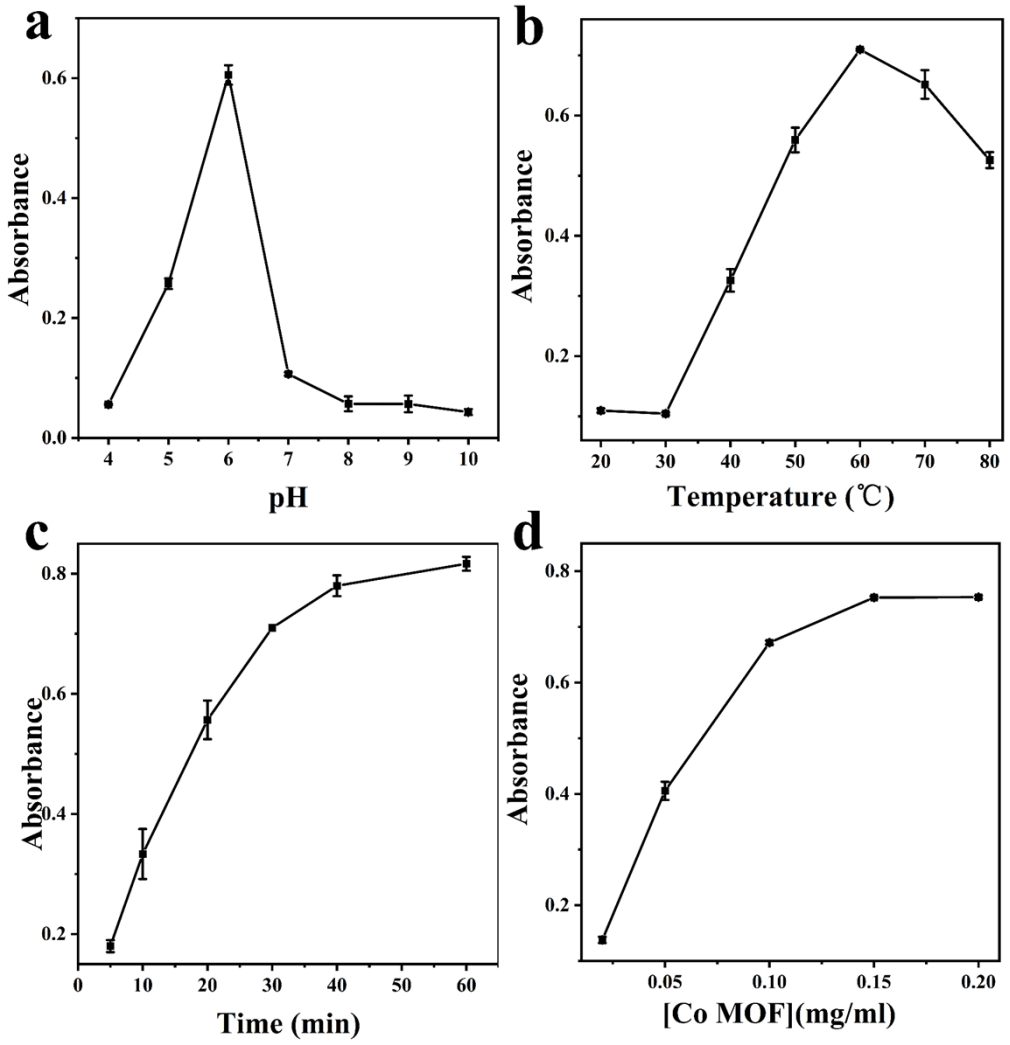

Fig. S4 Absorbance changes of the reaction system under different pH (a), temperatures (b), time (c) and Co-2MI concentrations (d)

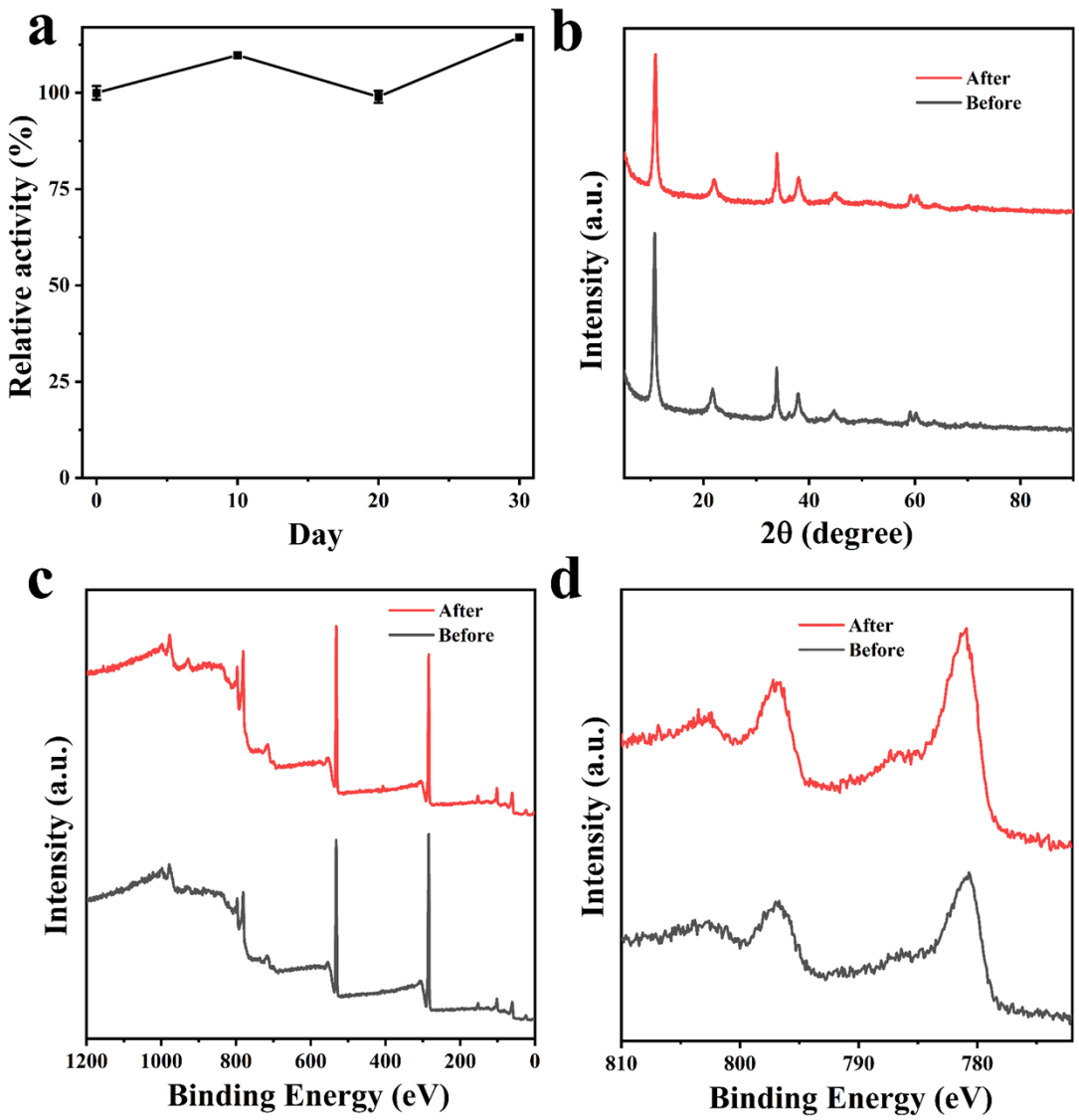

Fig. S5 (a) Activity comparison of Co-2MI during one month of room-temperature storage; XRD patterns (b), XPS survey spectra (c) and Co 2p XPS spectra (d) of Co-2MI before and after the reaction

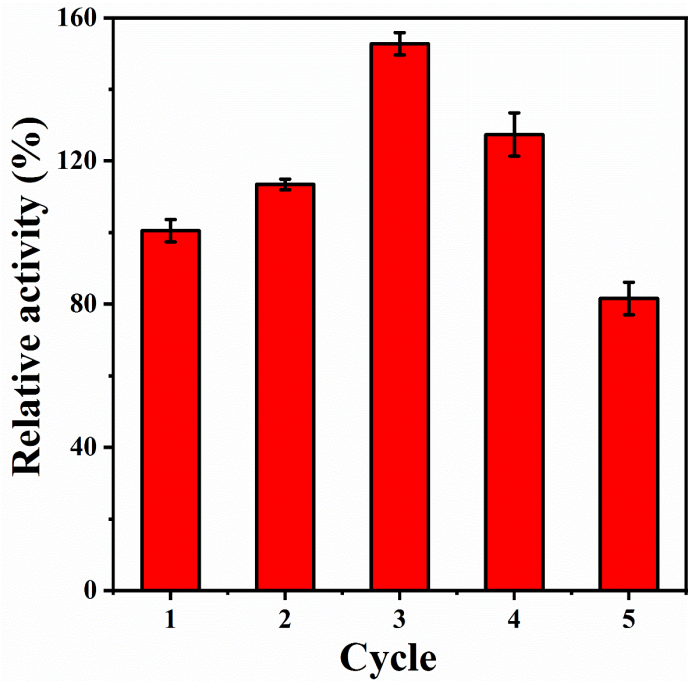

Fig. S6 Recycle performances of Co-2MI for the oxidation of 2,4-DP

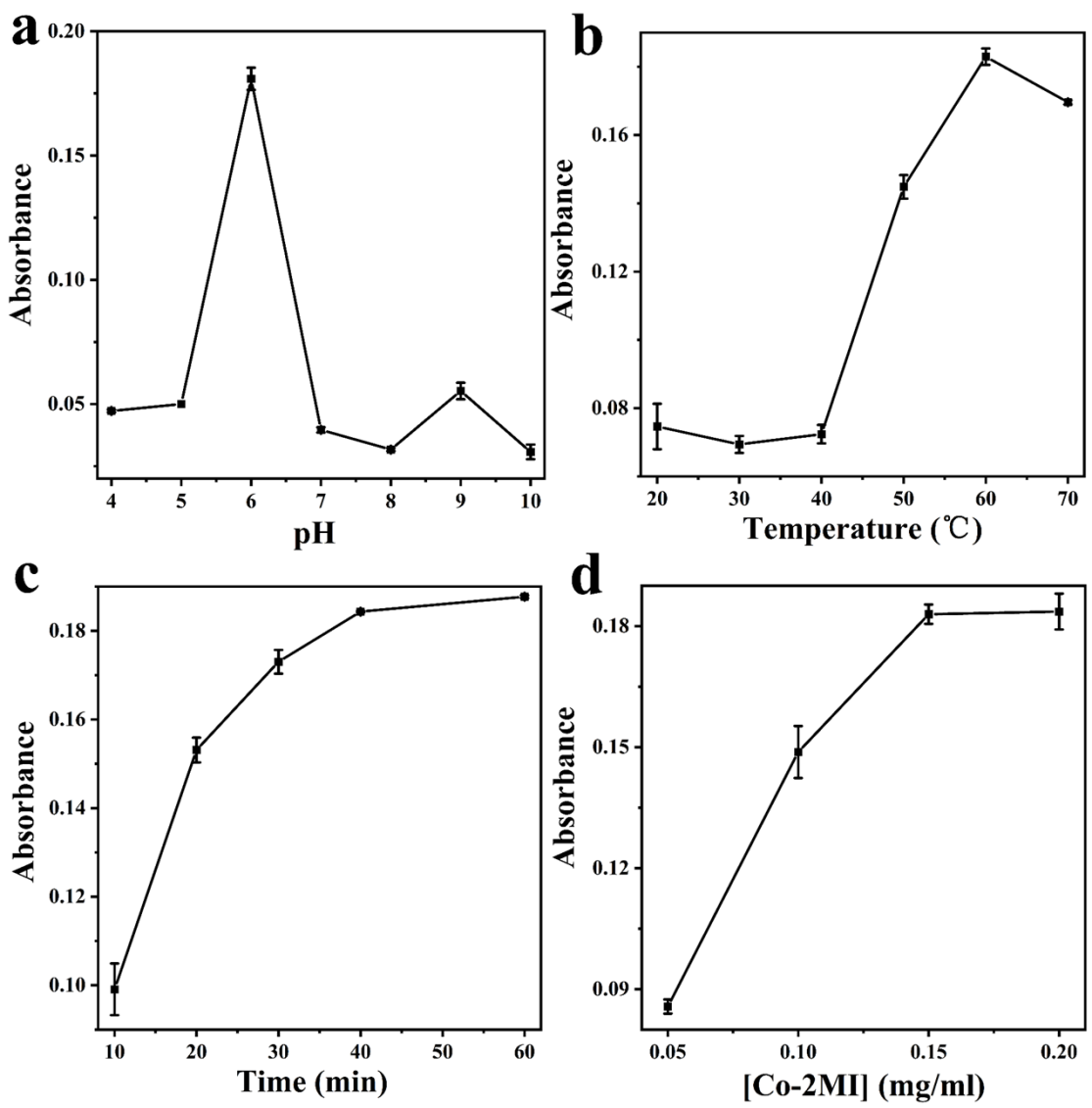

Fig. S7 Absorbance variation of the reaction system at different pH values (a), temperatures (b), time (c) and Co-2MI concentrations (d)

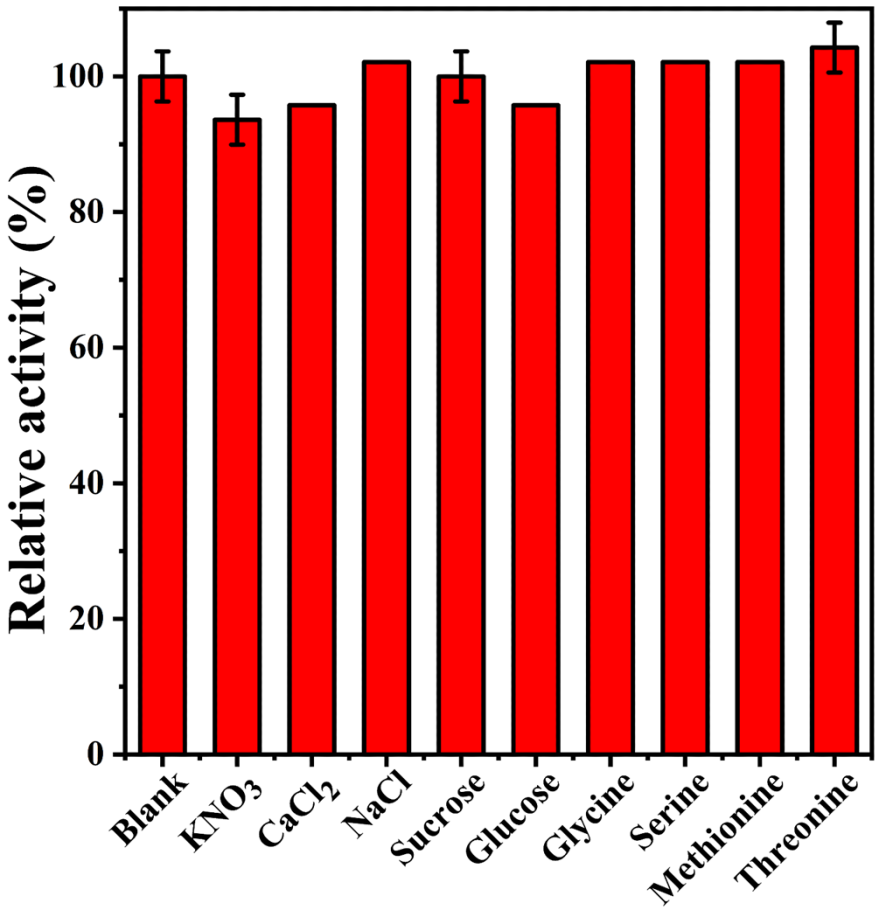

Fig. S8 Relative activity of Co-2MI in the presence of interfering substances

Table. S1 BET surface area and average pore diameter of the synthesized samples

	BET surface area (m^2 g^{-1})	Average pore diameter (nm)
Co-2MI	316.8	7.735
Co-BTC	164.1	6.095
Co-BDC	144.7	7.313
Co-BPDCA	60.62	5.037

References

1 Zhang D, Zhang H, Liu J A, Chen Y L, Bai J, Guo K, Cao D M and Zhou X M, *Mat. Sci. Eng. B-Adv.*, 2024, **307**, 117540.

2 Su L H, Chen J, Zhou J Z, Liu J J, Hu Z L, Li S, Hu X B, Xu L L and Zhang L, *Adv. Energy Mater.*, 2024, **14**, 2402489.

3 Abuzalat O, Tantawy H and Baraka A, *J. Water Process Eng.*, 2023, **54**, 103938.

4 Guo J W, Yang Z W, Liu X L, Zhang L W, Guo W B, Zhang J and Ding L H, *Rare Metals*, 2023, **42**, 797-805.

5 Liang H, Lin F F, Zhang Z J, Liu B W, Jiang S H, Yuan Q P and Liu J W, *Acs Appl Mater Inter*, 2017, **9**, 1352-1360.